CHAPTER

# Long and Medium Waves* 11

## 11.1 Introduction and equations

The main developments in this chapter relate to linearized surface waves in water, but acoustic and electromagnetic waves will also be mentioned. We start from the wave equation, Eq. (10.18), which was developed from the equations of momentum balance and mass conservation in shallow water. The wave elevation, $\eta$, is small in comparison with the water depth, $H$. If the problem is periodic, we can write the wave elevation, $\eta$, quite generally as

$$\eta(x, y, t) = \bar{\eta}(x, y)\exp(\mathrm{i}\omega t) \tag{11.1}$$

where $\omega$ is the angular frequency and $\bar{\eta}$ may be complex. Equation (10.18) now becomes

$$\nabla^{\mathrm{T}}\left(H\nabla\bar{\eta}\right) + \frac{\omega^2}{g}\bar{\eta} = 0 \quad \text{or} \quad \frac{\partial}{\partial x_i}\left(H\frac{\partial\bar{\eta}}{\partial x_i}\right) + \frac{\omega^2}{g}\bar{\eta} = 0 \tag{11.2}$$

or, for constant depth, $H$,

$$\nabla^2\bar{\eta} + k^2\bar{\eta} = 0 \quad \text{or} \quad \frac{\partial^2\bar{\eta}}{\partial x_i\,\partial x_i} + k^2\bar{\eta} = 0 \tag{11.3}$$

where the wavenumber $k = \omega/\sqrt{gH}$ is related to the wavelength, $\lambda$, by $k = 2\pi/\lambda$. The wave speed is $c = \omega/k$. Equation (11.3) is the Helmholtz equation [which was also derived in Chapter 10, in a slightly different form, as Eq. (10.18)] which models very many wave problems. This is only one form of the equation of surface waves, for which there is a very extensive literature [1–4]. From now on all problems will be taken to be periodic, and the overbar on $\eta$ will be dropped. The Helmholtz equation (11.3) also describes periodic acoustic waves. The wavenumber $k$ is now given by $\omega/c$, whereas in surface waves $\omega$ is the angular frequency and $c$ is the wave speed. This is given by $c = \sqrt{K/\rho}$, where $\rho$ is the density of the fluid and $K$ is the bulk modulus. Boundary conditions need to be applied to deal with radiation and absorption of acoustic waves. The first application of finite elements to acoustics was by Gladwell [5]. This was followed in 1969 by the solution of acoustic equations by Zienkiewicz and Newton [6], and further finite element models by Craggs [7].

*Contributed by Peter Bettess, Formerly Professor, School of Engineering, University of Durham, UK.

Finite Element Meth Fluid Dynam 7E, Volume 3. http://dx.doi.org/10.1016/B978-1-85617-635-4.00011-X

A more comprehensive survey of the development of the method is given by Astley [8]. Provided that the dielectric constant, $\varepsilon$, and the permeability, $\mu$, are constant, then Maxwell's equations for electromagnetics can be reduced to the form

$$\nabla^2\phi - \frac{\varepsilon\mu}{c^2}\frac{\partial^2\phi}{\partial t^2} = -\frac{4\pi\rho}{\varepsilon} \quad \text{and} \quad \nabla^2\mathbf{A} - \frac{\varepsilon\mu}{c^2}\frac{\partial^2\mathbf{A}}{\partial t^2} = -\frac{4\pi\mu\mathbf{J}}{c} \tag{11.4}$$

where $\rho$ is the charge density, $\mathbf{J}$ is the current, and $\phi$ and $\mathbf{A}$ are scalar and vector potentials, respectively. When $\rho$ and $\mathbf{J}$ are zero, which is a frequent case, and the time dependence is harmonic, Eqs. (11.4) reduce to the Helmholtz equations. More details are given by Morse and Feshbach [9].

For surface waves on water when the wavelength, $\lambda = 2\pi/k$, is small relative to the depth, $H$, the velocities and the velocity potential vary vertically as $\cosh kz$ [1,2,10,11]. The full equation can now be written as

$$\nabla^{\mathrm{T}}(cc_g\nabla\eta) + \frac{\omega^2}{g}\eta = 0 \quad \text{or} \quad \frac{\partial}{\partial x_i}\left(cc_g\frac{\partial\eta}{\partial x_i}\right) + \frac{\omega^2}{g}\eta = 0 \tag{11.5}$$

where the group velocity, $c_g = nc$, $n = (1+(2kH/\sinh 2kH))/2$, and the *dispersion relation*

$$\omega^2 = gk \tanh kH \tag{11.6}$$

links the angular frequency, $\omega$, and the water depth, $H$, to the wavenumber, $k$.

## 11.2 Waves in closed domains: Finite element models

We now consider a closed domain of any shape. For waves on water this could be a closed basin, for acoustic or electromagnetic waves it could be a resonant cavity. In the case of surface waves we consider a two-dimensional basin, with varying depth. In plan it can be divided into two-dimensional elements, of any of the types discussed in Ref. [12]. The wave elevation, $\eta$, at any point $(\xi, \eta)$ within the element, can be expressed in terms of nodal values, using the element shape function $\mathbf{N}$, as follows:

$$\eta \approx \hat{\eta} = \mathbf{N}\tilde{\eta} \tag{11.7}$$

Next Eq. (11.2) is weighted with the shape function, and integrated by parts in the usual way, to give

$$\int_\Omega \left(\frac{\partial\mathbf{N}}{\partial x_i}^T H \frac{\partial\mathbf{N}}{\partial x_i} - \mathbf{N}^{\mathrm{T}}\frac{\omega^2}{g}\mathbf{N}\right) \mathrm{d}\Omega\tilde{\eta} = 0 \tag{11.8}$$

The integral is taken over all the elements of the domain, and $\tilde{\eta}$ represents all the nodal values of $\eta$.

The natural boundary condition which arises is $\partial\eta/\partial n = 0$, where $n$ is the normal to the boundary, corresponding to zero flow normal to the boundary. Physically this corresponds to a vertical, perfectly reflecting wall. Equation (11.8) can be recast in the familiar form

$$(\mathbf{K} - \omega^2 \mathbf{M})\tilde{\eta} = \mathbf{0} \tag{11.9}$$

where

$$\mathbf{M} = \int_\Omega \mathbf{N}^\mathrm{T} \frac{1}{g} \mathbf{N}\, \mathrm{d}\Omega \quad \mathbf{K} = \int_\Omega \mathbf{B}^\mathrm{T} \mathbf{D} \mathbf{B}\, \mathrm{d}\Omega \tag{11.10}$$

and the **D** matrix is constructed from the depths, $H$. $H$ can vary with position:

$$\mathbf{D} = \begin{bmatrix} H & 0 \\ 0 & H \end{bmatrix}$$

It is thus an *eigenvalue* problem as discussed in Chapter 12 of Ref. [12]. The **K** and **M** matrices are analogous to structure stiffness and mass matrices. The *eigenvalues* will give the natural frequencies of oscillation of the water in the basin and the *eigenvectors* give the mode shapes of the water surface. Such an analysis was first carried out using finite elements by Taylor et al. [13] and the results are shown as Fig. 12.5 of Ref. [12]. There are analytical solutions for harbors of regular shape and constant depth [1,3]. The reader should find it easy to modify the standard element routine contained in the computer program available from the website given in Chapter 18 of Ref. [12] to generate the wave equation "stiffness" and "mass" matrices. In the corresponding acoustic problems, the eigenvalues give the natural resonant frequencies and the eigenvectors give the modes of vibration. The model described above will give good results for harbor and basin resonance problems, and other problems governed by the Helmholtz equation. In modeling the Helmholtz equation, it is necessary to retain a mesh which is sufficiently fine to ensure an accurate solution. A "rule of thumb," which has been used for some time, is that there should be 10 nodes per wavelength. This has been accepted as giving results of acceptable engineering accuracy for many wave problems. However, recently more accurate error analysis of the Helmholtz equation has been carried out [14,15]. In wave problems it is not sufficient to use a fine mesh only in zones of interest. The entire domain must be discretized to a suitable element density. There are essentially two types of errors:

- The wave shape may not be a good representation of the true wave, that is the local elevations or pressures may be wrong.
- The wavelength may be in error.

This second case causes a poor representation of the wave in one part of the problem to cause errors in another part of the problem. This effect, where errors build up across the model, is called a *pollution error*. It has been implicitly understood since the early days of modeling of the Helmholtz equation, as can be seen from the uniform size of finite element used in meshes.

Babuška et al. [14,15] show some results for various finite element models, using different element types, and the error is calculated as a function of element size, $h$, and wavenumber, $k$. The sharper error results show that the simple rule of thumb given above is not always adequate. Since the wavenumber, $k$, and the wavelength, $\lambda$, are related by $k = 2\pi/\lambda$, the condition of 10 nodes per wavelength can be written as $kh \approx 0.6$. But keeping to this limit is not sufficient. The pollution error grows as $k^3h^2$. Babuška et al. propose *a posteriori* error indicators to assess the pollution error. See the cited references and Chapter 15, Ref. [12], for further discussion of these matters.

## 11.3 Difficulties in modeling surface waves

The main defects of the simple surface-wave model described above are the following:

1. Inaccuracy when the wave height becomes large. The equations are no longer valid when $\eta$ becomes large, and for very large $\eta$, the waves will break, which introduces energy loss.
2. Lack of modeling of bed friction. This will be discussed below.
3. Lack of modeling of separation at re-entrant corners. At re-entrant corners there is a singularity in the velocity of the form $1/\sqrt{r}$, where $r$ is the distance from the corner. The velocities become large, and physically the viscous effects, neglected above, become important. They cause retardation, flow separation, and eddies. This effect can only be modeled in an approximate way.

Now the response can be determined for a given excitation frequency, as discussed in Chapter 12 of Ref. [12].

## 11.4 Bed friction and other effects

The engineering approach to the energy loss in the boundary layer close to the sea bed is to introduce a friction force proportional to the water velocity. This is called the Chézy bed friction. Since the force is nonlinear in the velocity if it is included in its original form, it makes the equations difficult to solve. The usual procedure is to assume that its main effect is to damp the system, by absorbing energy, and to introduce a linear term, which in one period absorbs the same amount of energy as the Chézy term. The linearized bed friction version of Eq. (11.2) is

$$\nabla^{\mathrm{T}}(H\nabla\eta) + \frac{\omega^2}{g}\eta - \mathrm{i}\omega M\eta = 0 \quad \text{or} \quad \frac{\partial}{\partial x_i}\left(H\frac{\partial\eta}{\partial x_i}\right) + \frac{\omega^2}{g}\eta - \mathrm{i}\omega M\eta = 0 \tag{11.11}$$

where $M$ is a linearized bed friction coefficient, which can be written as $M = 8u_{\max}/3\pi C^2 H$, $C$ is the Chézy constant, and $u_{\max}$ is the maximum velocity at the bed at that point. In general the results for $\eta$ will now be complex, and iteration has to be used, since $M$ depends upon the unknown $u_{\max}$. From the finite element point of view, there is no longer any need to separate the "stiffness" and "mass" matrices. Instead, Eq. (11.11) is weighted using the element shape function and the entire complex element matrix is formed. The matrix right-hand side arises from whatever exciting forces are present. The re-entrant corner effect and wave-absorbing walls and permeable breakwaters can also be modeled in a similar way, as both of these introduce a damping effect, due to viscous dissipation. The method is explained in Ref. [16], where an example showing flow through a perforated wall in an offshore structure is solved.

## 11.5 The short-wave problem

Short-wave diffraction problems are those in which the wavelength is much smaller than any of the dimensions of the problem. Such problems arise in surface waves on water, acoustic and pressure waves, electromagnetic waves, and elastic waves. The methods described in this chapter will solve the problems, but the requirement of 10 nodes or thereabouts per wavelength makes the necessary finite element meshes prohibitively fine. To take one example, radar waves of wavelength 1 mm might impinge on an aircraft of 10 m wingspan. It is easy to see that the computing requirements are truly astronomical. This topic is considered in more detail in Chapter 12.

## 11.6 Waves in unbounded domains (exterior surface wave problems)

Problems in this category include the diffraction and refraction of waves close to fixed and floating structures, the determination of wave forces and wave response for offshore structures and vessels, and the determination of wave patterns adjacent to coastlines, open harbors, and breakwaters. In electromagnetics there are scattering problems of the type already described, and in acoustics we have various noise problems. In the interior or finite part of the domain, finite elements, exactly as described in Section 11.2, can be used, but special procedures must be adopted for the part of the domain extending to infinity. The main difficulty is that the problem has no outer boundary. This necessitates the use of a *radiation condition*. Such a condition was introduced in Chapter 18 of Ref. [17] as Eq. (18.18) for the case of a one-dimensional wave, or a normally incident plane wave in two or more dimensions. Work by Bayliss et al. [18,19] has developed a suitable radiation condition, in the form of an infinite series of operators. The starting point is the representation of the outgoing wave in the form of an infinite series. Each term in the series is then annihilated by using a boundary operator. The sequence of boundary operators thus constitutes the radiation condition. In addition there is a classical form of the boundary condition for periodic problems, given by Sommerfeld [20,21]. A summary of some of the available radiation conditions is given in Table 11.1.

### 11.6.1 Background to wave problems

The simplest type of exterior, or unbounded wave problem is that of some exciting device which sends out waves which do not return. This is termed the *radiation* problem. The next type of exterior wave problem is where we have a known incoming wave which encounters an object, is modified, and then again radiates away to infinity.

**Table 11.1** Radiation Conditions for Exterior Wave Problems

| Dimensions | | |
|---|---|---|
| **1** | **2** | **3** |
| ***General boundary conditions*** | | |
| *Transient* | | |
| $\frac{\partial\phi}{\partial x}+\frac{1}{c}\frac{\partial\phi}{\partial t}=0$ | $B_m\phi=0, m\to\infty$ <br> $B_m=\prod_{j=1}^{m}\left(\frac{\partial}{\partial r}+\frac{\partial}{\partial t}+\frac{2j-(3/2)}{r}\right)$ | $B_m\phi=0, m\to\infty$ <br> $B_m=\prod_{j=1}^{m}\left(\frac{\partial}{\partial r}+\frac{\partial}{\partial t}+\frac{2j-1}{r}\right)$ |
| *Periodic* | | |
| $\frac{\partial\phi}{\partial x}+\mathrm{i}k\phi=0$ | $\lim_{r\to\infty}\sqrt{r}\left(\frac{\partial\phi}{\partial r}+\mathrm{i}k\phi\right)=0$ <br> or <br> $B_m\phi=0, m\to\infty$ <br> $B_m=\prod_{j=1}^{m}\left(\frac{\partial}{\partial r}+\mathrm{i}k+\frac{2j-(3/2)}{\gamma}\right)$ | $\lim_{r\to\infty}r\left(\frac{\partial\phi}{\partial r}+\mathrm{i}k\phi\right)=0$ <br> or <br> $B_m\phi=0, m\to\infty$ <br> $B_m=\prod_{j=1}^{m}\left(\frac{\partial}{\partial r}+\mathrm{i}k+\frac{2j-1}{r}\right)$ |
| ***Symmetric boundary conditions*** | | |
| *Transient* | | |
| $\frac{\partial\phi}{\partial r}+\frac{1}{c}\frac{\partial\phi}{\partial t}=0$ | $\frac{\partial\phi}{\partial r}+\frac{\phi}{2r}+\frac{1}{c}\frac{\partial\phi}{\partial t}=0$ <br> Axisymmetric | $\frac{\partial\phi}{\partial r}+\frac{\phi}{r}+\frac{1}{c}\frac{\partial\phi}{\partial t}=0$ <br> Spherically symmetric |
| *Periodic* | | |
| $\frac{\partial\phi}{\partial r}+\mathrm{i}k\phi=0$ | $\frac{\partial\phi}{\partial r}+\left(\frac{1}{2r}+\mathrm{i}k\right)\phi=0$ <br> Axisymmetric | $\frac{\partial\phi}{\partial r}+\left(\frac{1}{r}+\mathrm{i}k\right)\phi=0$ <br> Spherically symmetric |

This case is known as the *scattering* problem, and is more complicated, inasmuch as we have to deal with both incident and radiated waves. Even when both waves are linear, this can lead to complications. Both the above cases can be complicated by wave refraction, where the wave speeds change, because of changes in the medium, for example changes in water depth. Usually this phenomenon leads to changes in the wave direction. Waves can also reflect from boundaries, both physical and computational.

### 11.6.2 Wave diffraction

We now consider the problem of an incident wave diffracted by an object. The problem consists of an object in some medium, which diffracts the incident waves. We divide

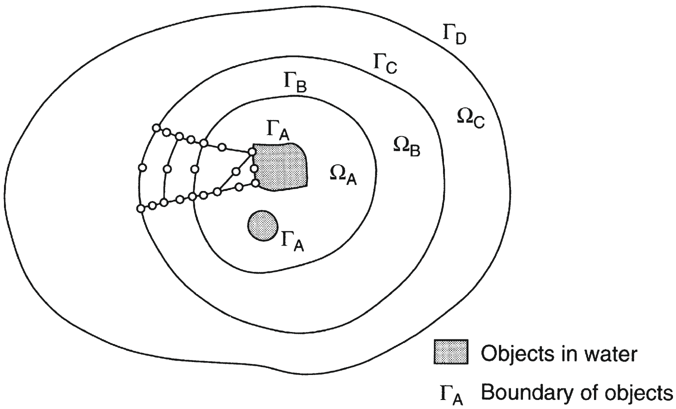


**FIGURE 11.1**
General wave domains.

the medium as shown in Fig. 11.1, into two regions, with boundaries $\Gamma_A$, $\Gamma_B$, $\Gamma_C$, and $\Gamma_D$. These boundaries have the following meanings. $\Gamma_A$ is the boundary of the body which is diffracting the waves. $\Gamma_B$ is the boundary between the two computational domains, that in which the total wave elevation (or other field variable) is used, and that in which the elevation of the radiated wave is used. $\Gamma_C$ is the outer boundary of the computational model, and $\Gamma_D$ is the boundary at infinity. Some of these boundaries may be merged.

A variational treatment will now be used, as described in Chapters 3 and 4 of Ref. [12]. A weighted residual treatment is also possible. The elevation of the total wave, $\eta_T$, is split into those for incident and radiated waves, $\eta_I$ and $\eta_R$. Hence $\eta_T = \eta_I + \eta_R$. The incident wave elevation, $\eta_I$, is assumed to be known. For the surface wave problem, the functional for the exterior can be written as

$$\Pi = \iint_{\Omega_B} \frac{1}{2}\left[cc_g(\nabla\eta)^{\mathrm{T}}\nabla\eta - \frac{\omega^2 c_g}{c}\eta^2\right]\mathrm{d}x\,\mathrm{d}y \tag{11.12}$$

where making $\Pi$ stationary with respect to variations in $\eta$ corresponds to satisfying the shallow-water wave equation (11.5), with natural boundary condition $\partial\eta/\partial n = 0$, or zero velocity normal to the boundary. The functional is rewritten in terms of the incident and radiated elevations, and then Green's theorem in the plane (Ref. [12], Appendix F) is applied on the domain exterior to $\Gamma_B$. But the radiation condition discussed above should be included. In order to do this the variational statement must be changed so that variations in $\eta$ yield the correct boundary condition. Details are given by many authors, see for example Bettess and Bettess [22]. After some manipulation the final functional for the exterior is

$$\Pi = \iint_{\Omega_b} \frac{1}{2}\left[cc_g(\nabla\eta^s)^T\nabla\eta^s - \frac{\omega^2 cc_g}{c}(\eta^s)^2\right]\mathrm{d}x\,\mathrm{d}y$$
$$+ \int_{\Gamma_b} cc_g\left[\frac{\partial\eta^i}{\partial x}\eta^s\,\mathrm{d}y - \frac{\partial\eta^i}{\partial y}\eta^s\,\mathrm{d}x\right] + \frac{1}{2}\int_{\Gamma_d} \mathrm{i}kcc_g(\eta^s)^2\,\mathrm{d}\Gamma \tag{11.13}$$

The influence of the incident wave is thus to generate a "forcing term" on the boundary $\Gamma_B$. For two of the most popular methods for dealing with exterior problems, linking to boundary integrals and infinite elements, the "damping" term in Eq. (11.13), corresponding to the radiation condition, is actually irrelevant, because both methods use functions which automatically satisfy the radiation condition at infinity.

### 11.6.3 Incident waves, domain integrals, and nodal values

It is possible to choose any known solution of the wave equation as the incident wave. Usually this is a plane monochromatic wave, for which the elevation is given by $\eta_I = a_0 \exp[ikr\cos(\theta - \gamma)]$, where $\gamma$ is the angle that the incident wave makes to the positive $x$-axis, $r$ and $\theta$ are the polar coordinates, and $a_0$ is the incident wave amplitude. On the boundary $\Gamma_B$, we have two types of variables, the total elevation, $\eta_T$, on the interior, and $\eta_R$, the radiation elevation, in the exterior. Clearly the nodal values of $\eta$ in the finite element model must be unique, and on this boundary, as well as the line integral, of Eq. (11.13), we must transform the nodal values, either to $\eta_T$ or to $\eta_R$. This can be done simply by enforcing the change of variable, which leads to a contribution to the "right-hand side" or "forcing" term [22].

## 11.7 Unbounded problems

There are several methods of dealing with exterior problems using finite elements in combination with other methods. Some of these methods are also applicable to finite differences. The literature in this field has grown enormously in the past few years, and this section cannot begin to pretend to be comprehensive. A book could be written on each of the subheadings below. The monograph by Givoli [23] is devoted exclusively to this field and gives much more detail on the competing algorithms. It is a very useful source and gives many more algorithms than can be covered here. The book edited by Geers [24], from an IUTAM symposium, gives a very useful and up-to-date overview of the field. Methods for exterior Helmholtz problems are also discussed by Ihlenburg in his monograph [25].

Four of the main methods are listed below. The first three are usually local in their effect. The last is always global, linking together all the nodes on the exterior of the finite element mesh.

- Local nonreflecting boundary conditions (NRBCs)
- *Sponge layers*, perfectly matched layers (PMLs)
- Infinite elements

- Linking to exterior solutions, both series and boundary integrals [also called Dirichlet to Neumann mapping (DtN)].

## 11.8 Local nonreflecting boundary conditions (NRBCs)

The term comes from the mathematical literature. These conditions are also called boundary dampers by engineers because of the obvious physical analogy. As was seen in Chapter 12 of Ref. [12], we can simply apply the plane damper at the boundary of the mesh. This was first done in fluid problems by Zienkiewicz and Newton [6]. However the low-order versions of the more sophisticated NRBCs or dampers proposed by Baylisss et al. [18,19] can be used at little extra computational cost and a big increase in accuracy. The NRBCs are developed from the series given in Table 11.1. Details for low-order cases are given in Ref. [26]. For the case of two-dimensional waves the line integral which should be applied on the circular boundary of radius $r$ is

$$A = \int_{\Gamma} \left[ \frac{\alpha}{2}\eta^2 + \frac{\beta}{2}\left(\frac{\partial \eta}{\partial s}\right)^2 \right] \mathrm{d}s \tag{11.14}$$

where $\mathrm{d}s$ is an element of distance along the boundary and

$$\alpha = \frac{3/4r^2 - 2k^2 + 3\mathrm{i}k/r}{2/r + 2\mathrm{i}k} \quad \text{and} \quad \beta = \frac{1}{2/r + 2\mathrm{i}k} \tag{11.15}$$

For the plane damper, $\beta = 0$ and $\alpha = \mathrm{i}k$. For the cylindrical damper $\beta = 0$ and $\alpha = \mathrm{i}k - 1/2r$. The corresponding expressions for three-dimensional waves are different. Noncircular boundaries can be handled but the expressions become much more complicated. This is because as the higher-order terms are included in the boundary condition, then higher-order derivatives in the normal direction are required. These can be transformed into derivatives in the circumferential direction by using the governing wave equation. However, even derivatives in the circumferential direction pose difficulties. So NRBCs based on the Bayliss expressions have, in practice, been limited to the lowest few terms. Some results are given by Bando et al. [26]. Figure 11.2 shows the waves diffracted by a cylinder problem for which there is a solution, due to Havelock [27]. In this case the second-order damper is the highest order modeled. The higher-order dampers are clearly a big improvement over the plane and cylindrical dampers, for little or no extra computational cost. Other researchers, of whom we mention only Engquist and Majda [28,29], Higdon [30,31], and Hagstrom et al. [32,33], have also proposed NRBCs. Although the derivations vary considerably the effect is similar, in that a hierarchy of boundary operators is defined, but the resulting terms are different to those of Bayliss et al.

For the Helmholtz equation the general form of these NRBCs can be written as

$$\prod_{j=1}^{N} \left( \frac{\partial}{\partial t} + C_j \frac{\partial}{\partial n} \right) \phi = 0 \tag{11.16}$$

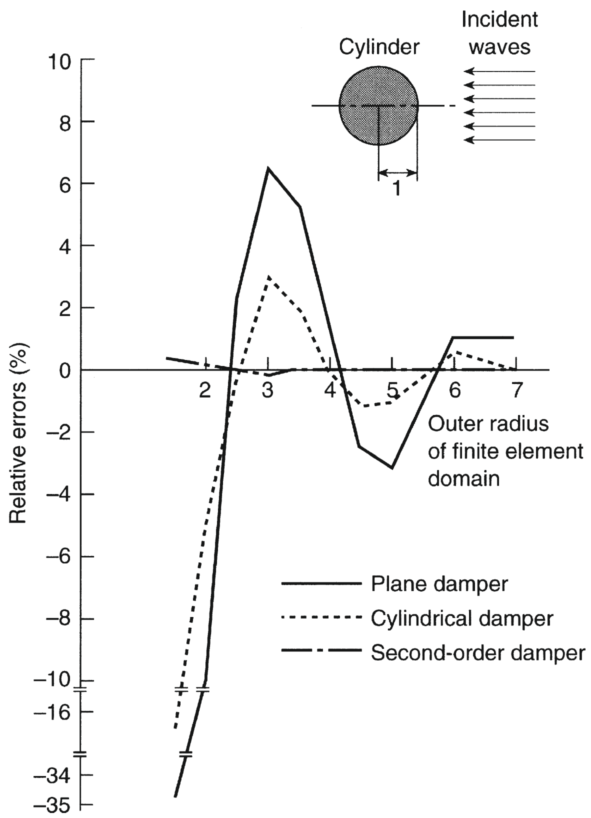


**FIGURE 11.2**

Damper solutions for waves diffracted by circular cylinder. Comparison of relative errors for various outer radii ($ka = 1$). Relative error $= (abs(\eta_n) - abs(\eta_a))/abs(\eta_a)$.

where $\phi$ is the field variable, $n$ is the normal to the boundary, and $C_j$ is the $j$ term in the boundary condition. The expressions for $C_j$ vary, depending upon whose theory is used. One approach is simply to use a range of waves with different angles of incidence. (Obviously the plane damper case arises when $N = 1$ and $C_1$ is the wave speed.) All these sets of NRBCs have in common the problem of the escalating order of derivatives, arising from expansion of the products of the operator terms in Eq. (11.16). This has been a problem but Givoli [34,35] has recently demonstrated how the high-order derivative difficulty can be sidestepped through the use of auxiliary variables. The most straightforward way of using auxiliary variables leads to an unsymmetric matrix for the boundary condition terms. But Givoli [35] proves that this unsymmetric matrix can always be transformed into a symmetric form and gives the necessary construction. The method results in the addition of auxiliary variables on the boundary of the mesh, but no other difficulties. Givoli expands Eq. (11.16), using auxiliary variables so that it becomes

$$\left(\frac{\partial}{\partial t}+C_j\frac{\partial}{\partial n}\right)\phi = u_1 \tag{11.17}$$

$$\left(\frac{\partial}{\partial t}+C_j\frac{\partial}{\partial n}\right)u_1 = u_2 \tag{11.18}$$

$$\vdots$$

$$\left(\frac{\partial}{\partial t}+C_j\frac{\partial}{\partial n}\right)u_{N-1} = u_N \tag{11.19}$$

where $u_j$ are the auxiliary variables. The resulting matrix (which in general is unsymmetric), representing the effect of these auxiliary variables on the boundary, is then transformed according to Givoli's procedure into a symmetrical matrix. The procedure works for both transient and harmonic problems.

The literature on these boundary conditions has grown remarkably in recent years and this section has only been able to give an outline of the possibilities available. For further information the reader is referred to the book by Givoli [23] and the volume edited by Geers [24], which gives access to recent developments. The papers in the Geers volume by Bielak, Givoli, Hagstrom, Hariharan, Higdon, Pinsky, and Kallivokas should be consulted.

### 11.8.1 Sponge layers or perfectly matched layers (PMLs)

As was seen earlier, nonreflecting boundary conditions (NRBCs) attempt to absorb the outgoing wave on the boundary of the computational domain. An obvious extension of this idea is to absorb the wave over an artificial domain, external to the domain of interest. It is intuitively obvious that if the domain is made large enough and the correct damping is inserted, then the wave energy reflected back into the domain of interest must become very small. In surface waves the physical analogy is to the energy absorbers, often made of horse hair, at the ends of wave tanks. The theoretical developments in this field go under two names, *sponge layer* which tends to be used in hydraulic computations and meteorology and *perfectly matched layers* (PMLs), in electromagnetics, or Maxwell's equations, and related fields such as acoustics, quantum mechanics, and elastodynamics. Some authors do use both terms. The first paper on the method appears to be that of Larsen and Dancy [36] in 1983. The PML was first applied to Maxwell's equations by Bérenger [37,38], in 1994. In this method a damping factor is introduced in each equation in those places where a normal spatial derivative appears. That is the governing equations are modified so that in the sponge layer or PML region a damping term is introduced. The damping factor is selected in a semi-empirical way and typically varies in space. More details are given in Refs. [39,40] and in the papers by Monk and Collino, Hayder, and Driscoll in Ref. [24].

## 11.9 Infinite elements

Infinite elements are described in the book by Bettess [41], which although out-of-date, can be used as an introduction to the topic. More recent reviews are by Astley [42] and Gerdes [43]. The methods described Chapter 7 of Ref. [12], can be developed to include periodic effects. This was first done by Bettess and Zienkiewicz, using so-called "decay function" procedures and they were very effective [11,44]. Comparison results with Chen and Mei [45,46] for the artificial island problem are shown in Fig. 12.6 of Ref. [12]. Later "mapped" infinite elements were developed for wave problems, and as these are more accurate than those using exponentials, they will be described here.

### 11.9.1 Mapped periodic (unconjugated) infinite elements

The theory developed in Chapter 7 of Ref. [12] for static infinite elements will not be repeated here. Details are given in Refs. [11,22,41–44,47–51]. Finite element polynomials of the form

$$P = \alpha_0 + \alpha_1 \xi + \alpha_2 \xi^2 + \cdots \quad \text{become} \quad P = \beta_0 + \frac{\beta_1}{r} + \frac{\beta_2}{r^2} + \cdots \tag{11.20}$$

in which $\beta_i$ can be determined from the $\alpha$'s and $a$. If the polynomial is zero at infinity then $\beta_0 = 0$.

Many exterior wave problems have solutions in which the wave amplitude decays radially like $1/r$ (and higher-order terms) and an advantage of this mapping is that such a decay can be represented exactly. In some cases, however, the amplitude decays approximately as $1/\sqrt{r}$, and this case needs a slightly different treatment. Accuracy can be increased by adding extra terms to the series (11.20).

#### *11.9.1.1 Introducing the wave component*

In two-dimensional exterior domains the solution to the Helmholtz equation can be described by a series of combined Hankel and trigonometric functions, the simplest solution to the Helmholtz equation being $H_0(kr)$. For large $r$ the zeroth-order Hankel function oscillates roughly like $\cos(kr) + \mathrm{i}\sin(kr)$, while decaying in magnitude as $r^{-1/2}$. A series of terms $1/r$, $1/r^2$, etc., generated by the mapping, multiplied by $r^{1/2}$ and the periodic component $\exp(\mathrm{i}kr)$ will be used to model the $r^{-1/2}$ decay. The shape function is thus

$$N(\xi, \eta) = M(\xi, \eta) r^{1/2} \exp(\mathrm{i}kr) \tag{11.21}$$

where $r = A/(1-\xi)$. The shape function in Eq. (11.21) will now be, for compatibility with the finite elements,

$$N(\xi, \eta) = M(\xi, \eta) \left(\frac{2}{A}\right)^{1/2} \left(\frac{A}{1-\xi}\right)^{1/2} \exp\left(\frac{\mathrm{i}kA}{2}\right) \exp\left(\frac{\mathrm{i}kA}{1-\xi}\right) \tag{11.22}$$

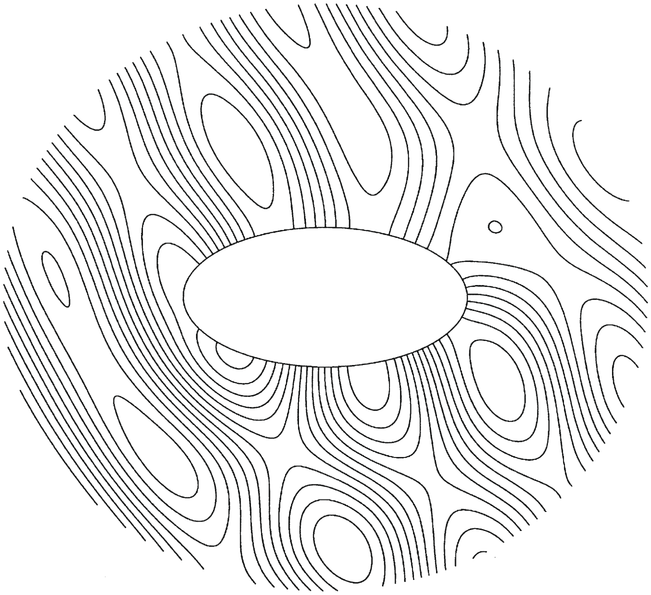

**FIGURE 11.3**

Real part of elevations of plane wave diffracted by an ellipse, of aspect ratio 2, Bettess [22].

In the improved version of this element [22], the constant, $A$, varies within the element. $A$ is now determined on each radial line from the positions of the nodes. It is interpolated between these values. The original mapped infinite element did not include the possibility of varying the mapping, so that the infinite elements had to be placed exterior to a cylinder or sphere. There was also an uncertainty about the integrations in the infinite radial direction, which was resolved by Astley et al. [51] This arose because the boundary terms at infinity were incompletely stated, although the element, as presented in Refs. [49,50], is correct. Following the introduction of a shape function of the form given in Eq. (11.22), the standard finite element methodology is used. That is to say the weighted residual or variational expression is formed and integrated over the infinite domain. The only novelties are the oscillatory nature of the shape function, and the infinite extent of the domain. Mapped wave envelope infinite elements were later developed, using the same methodology, but with a complex conjugate weighting (see Section 11.9.2). Later still Astley et al. [52], Cremers, and Fyfe and Coyette [53,54] generalized the mapping of these wave envelope infinite elements, so that it was no longer necessary to place them exterior to a sphere or cylinder. After this work Bettess and Bettess [22] generalized the original mapped wave infinite elements. Figure 11.3 shows some results from the diffraction of waves by an ellipse, for which there is an analytical solution.

### 11.9.2 Ellipsoidal type infinite elements of Burnett and Holford

Burnett with Holford [55–57] proposed a completely new type of infinite element for exterior acoustics problems. This uses prolate or oblate spheroidal coordinates, and separates the radial and angular coordinates. Burnett also further clarified the variational statement of the problem and explained in more detail the terms at the infinite boundary. It is known that a scattered wave exterior to a sphere can be written in spherical polar coordinates as

$$p = \frac{\mathrm{e}^{-kr}}{r} \sum_{n=0}^{\infty} \frac{G_n(\theta, \phi, k)}{r^n} \tag{11.23}$$

This proof was generalized to the case when the coordinates $\theta, \phi, r$ are not simply spherical, but prolate or oblate spheroidal or ellipsoidal. There are several benefits to using such coordinate systems:

- The volume integrals separate into radial and angular parts which can be carried out independently. This leads to economies in computation.
- The radial integration is identical for every such infinite element, so that the only integration which needs to be carried out for every infinite element is along the finite element interface.
- The radial integration is the only part containing the wavenumber.
- The ellipsoidal coordinates can be used to enclose a large variety of different geometries in the finite element interior, while still retaining a guarantee of convergence in 3D.

The angular shape functions are written in the conventional polynomial form. The radial shape functions take the form

$$N_i = \mathrm{e}^{-\mathrm{i}kr} \sum_{j=1}^{m} \frac{h_{ij}}{(kr)^j} \tag{11.24}$$

The coefficients $h_{ij}$ are given from the condition of circumferential compatibility between adjacent infinite elements. There is effectively no difference between this radial behavior and that originally proposed in the mapped infinite wave elements by Bettess et al. [49,50]. The difference in the infinite element methodology lies in the fact that the radial variable, $r$, is now in ellipsoidal coordinates. Burnett and Holford [55–57] give the necessary detailed information for the element integrations and the programming of these infinite elements, together with some results. The analytical expressions are too long to include here. The elements have been used on submarine fluid-structure interaction problems, and substantial efficiencies over the use of boundary integral models for the scattered waves have been claimed. In one case Burnett states that the finite and infinite element model ran for 7 h on a workstation. His projected time for the corresponding boundary element model was about 3000 h, the infinite elements giving a dramatic improvement!

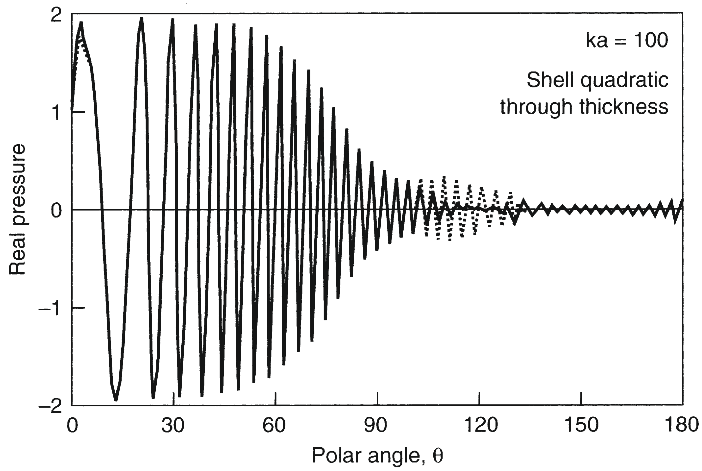


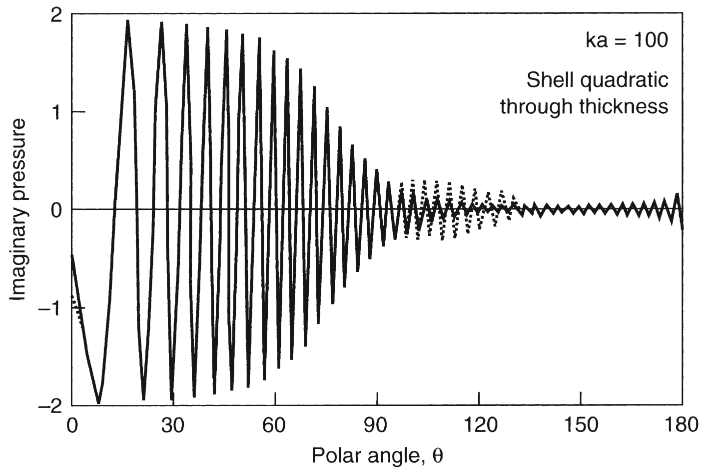


**FIGURE 11.4**

Waves scattered by an elastic sphere for $ka = 100$, Burnett and Halford [57].

The Burnett elements have been tested up to very short-wave cases, up to $ka = 100$ for an elastic sphere diffraction problem, which is shown in Fig. 11.4.

### 11.9.3 Wave envelope (or conjugated) infinite elements

Astley introduced a new type of finite element, in which the weighting function is the complex conjugate of the shape function [58,59]. The great simplification which this introduces is that the oscillatory function $\exp(ikr)$ cancels after being multiplied by $\exp(-ikr)$, and the remaining terms are all polynomials, which can be integrated using standard techniques, like Gauss-Legendre integration (see Chapters 3 and 6 of Ref.

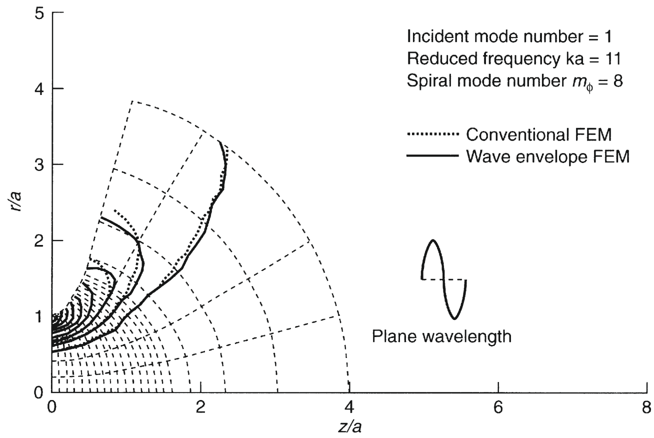


**FIGURE 11.5**

Computed acoustical pressure contours for a hyperbolic duct ($\theta_0 = 70°$, $ka = 11$, $m_\phi = 8$). Conventional and wave envelope element solutions, Astley [59].

[12]). This type of element was originally large (i.e., many wavelengths in extent), but not infinite. Figure 11.5 shows an example from acoustics, that of acoustical pressure in a hyperbolic duct. Good results were obtained despite using a relatively coarse mesh. Astley's shape function was of the form

$$N_i(r,\theta)\frac{r_i}{r}e^{-ik(r-r_i)} \tag{11.25}$$

where $N_i$ is the standard shape function. The weighting function is thus

$$N_i(r,\theta)\frac{r_i}{r}e^{ik(r-r_i)} \tag{11.26}$$

Bettess [60] showed that for a one-dimensional synthetic wave-type equation the infinite wave envelope element recovers the exact solution. The element matrix is now hermitian rather than symmetric (though still complex), which necessitates a small alteration to the equation solver. (There are not usually any problems in changing standard profile or front solvers to deal with complex systems of equations.) Unfortunately the problem tackled by Bettess did not include the essential feature of physical waves, in two and three dimensions. Later workers applied the wave envelope concept to true wave problems. In this case it can be shown that if the weighting function is simply the complex conjugate of the shape function, terms arise on the boundary at infinity.[1] This is discussed by Bettess [41]. The terms can be evaluated, but they are not symmetrical (or hermitian), and therefore impose a change of solution technique. An alternative, which eliminates the terms at infinity, was proposed by

[1] Some writers, particularly mathematicians, prefer to call the usual wave infinite elements unconjugated infinite elements, and the Astle-type wave envelope infinite elements conjugated infinite elements.

Astley et al. [52]. In this a "geometrical factor" is included in the weighting function, which then takes the form

$$N_i(r,\theta)\left(\frac{r_i}{r}\right)^3 \mathrm{e}^{\mathrm{i}k(r-r_i)} \tag{11.27}$$

It has been shown that this form of weighting functions gives very good results. Such wave envelope infinite elements have been further developed by Coyette, Cremers and Fyfe [53,54]. These elements have incorporated a more general mapping than that in the original Zienkiewicz et al. mapped infinite wave element. Cremers and Fyfe allow the mapping to vary in the local $\xi$ and $\eta$ directions.

### 11.9.4 Accuracy of infinite elements

The use of a complex conjugate weighting in the wave envelope infinite elements means that the original variational statement, Eq. (11.12), must be changed to allow the use of the different weighting function. This gives rise to a number of issues relating to the nature of the weighted residual statement and the existence of various terms. These issues were touched upon by Bettess [41], but have been subsequently subjected to more detailed study. Gerdes and Demkowitz [61,62] analyzed the wave envelope elements, and subsequently the wave infinite elements [63]. Some of this work is restricted to spherical scatterers. Other analysis is carried out by Shirron and Babuška [64,65], who reveal a somewhat paradoxical result. The original (unconjugated) infinite elements give better results in the finite element mesh, but worse results in the infinite elements themselves. But the wave envelope (conjugated) elements give worse results in the finite elements, and better results in the far field. This result, which is ascribed to ill-conditioning, does seem to be counterintuitive. Astley [42] and Gerdes [43] have also surveyed current formulations and accuracies. Infinite elements have traditionally been used with relatively small numbers of radial terms. Recent investigations have addressed the problems of ill-conditioning and accuracy of infinite elements when the number of terms in the radial direction is increased [42,66–68]. In general it is found that the more radial terms that are retained, the worse the conditioning of the infinite element. This is similar to the effect noted in plane wave basis finite elements, which are discussed in Chapter 12. It has been suggested by Dreyer and von Estorff [68] that the ill-conditioning effect can be reduced by the use of Jacobi polynomials in the radial direction.

### 11.9.5 Other applications

Infinite elements have been applied to a large range of applications, and it is impossible to survey the field in the scope of this chapter. The reader is directed to Refs. [41–43]. An interesting application of infinite elements to Maxwell's equations by Demkowitz and Pal [69] is worthy of mention.

### 11.9.6 Trefftz-type infinite elements

Harari, with various coworkers [70–73], has developed infinite elements for the Helmholtz equation in two and three dimensions. The elements are sectors, bounded by radial lines defined by $\theta_s$ and $\theta_{s+1}$, and the arc $r = R$. Then $\Delta\theta_s = \theta_{s+1} - \theta_s$. Hankel functions are used to describe the radial behavior and the circumferential behavior is modeled using linear polynomials in $\theta$. For a two-noded element the shape functions can be written

$$N_1 = \frac{H_0(kr)}{H_0(kR)}\frac{\theta_{s+1} - \theta}{\Delta\theta_s} \quad \text{and} \quad N_1 = \frac{H_0(kr)}{H_0(kR)}\frac{\theta - \theta_s}{\Delta\theta_s} \tag{11.28}$$

The advantage of this formulation is that because the Hankel functions are solutions of the Helmholtz equation the integrations over the infinite elements can be eliminated. Continuity between the finite element domain and the infinite element domain is enforced weakly, as is the continuity between adjacent infinite elements. Harari shows that the matrices which arise for the case of linear infinite elements, with an orientation as specified, are

$$kR\frac{H_0'(kR)}{H_0(kR)}\frac{\Delta\theta_s}{6}\begin{bmatrix} 2 & 1 \\ 1 & 2 \end{bmatrix} \tag{11.29}$$

for the finite/infinite element interface and

$$kR\frac{\alpha_{00}}{\Delta\theta_s}\begin{bmatrix} 1 & -1 \\ -1 & 1 \end{bmatrix} \tag{11.30}$$

where

$$\alpha_{00} = \int_0^\infty \frac{H_0(kr)H_0(kr)}{H_0(kR)H_0(kR)}\frac{dr}{r} \tag{11.31}$$

for the boundaries between the infinite element radial boundaries. He also goes on to develop higher-order infinite elements of similar type. He gives results for some academic type problems.

## 11.10 Convection and wave refraction

Conventional wave finite elements will deal satisfactorily with wave refraction caused by local changes in wave speed. This is seen in the example of Figure 11.6, where changes in water depth lead to local changes in wave speed. In exterior domains infinite elements have difficulties if the problem has a wave speed which is a function of position. There are also difficulties with linking to exterior solutions, or DtN methods, if an analytical solution or Green's function is used, since these almost invariably assume constant wave speed, in which case the Helmholtz equation is homogeneous.

However acoustic waves in inhomogeneous media have been solved using finite elements in conjunction with large (but finite) wave envelope elements by Astley

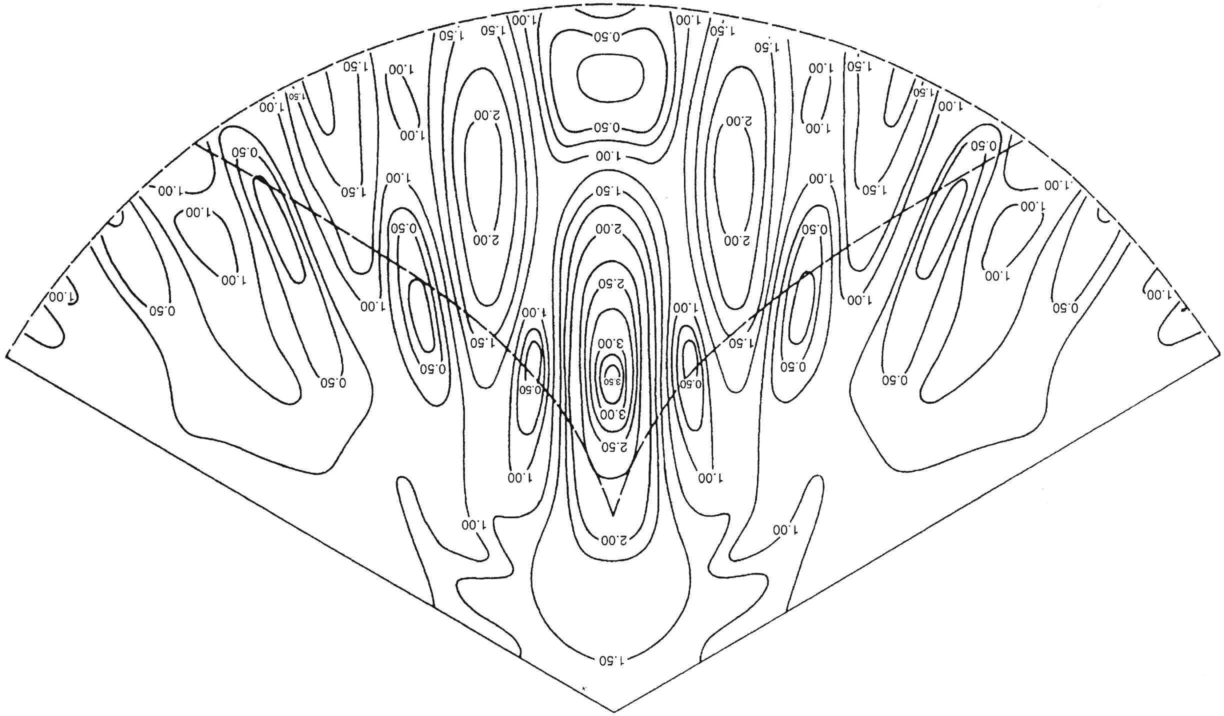

**FIGURE 11.6**
Refraction-diffraction solution: lines of equal wave height, lines every 0.25 unit [10].

and Eversman [74]. In this case the governing equation is the inhomogeneous wave equation

$$\rho\nabla \cdot \left(\frac{1}{\rho}\nabla p^*\right) - \left(1/c^2\right)\frac{\partial^2 p^*}{\partial t^2} = 0 \tag{11.32}$$

where $\rho$ is the density, $c$ is the wave speed, and $p^*$ is the acoustical pressure.

Wave refraction can also occur because the waves are superposed upon a underlying flow field. Important applications are surface waves on water currents and sound waves on air flows, for example in aircraft noise. This case is more difficult and the general equations become complicated. See for example, Lighthill [4]. For the case of sound waves superposed on a flow field Astley [75] has applied wave envelope finite elements to problems in which a substantial amount of convection is present. In this case the governing equation is no longer the Helmholtz equation. A detailed discussion is beyond the scope of this chapter.

## 11.11 Transient problems

Astley [76–78] has extended his wave envelope infinite elements using the prolate and oblate spheroidal coordinates adopted by Burnett and Holford [55–57], and has shown that they give accurate solutions to a range of transient wave problems. With the geometric factor of Astley, which reduces the weighting function and eliminates the surface integrals at infinity, the stiffness, **K**, damping, **C**, and mass, **M**, matrices of the wave envelope infinite element become well defined and *frequency independent*, although unsymmetric. This makes it possible to apply such elements to unbounded transient wave problems. Figure 11.7 shows the transient response of a dipole.

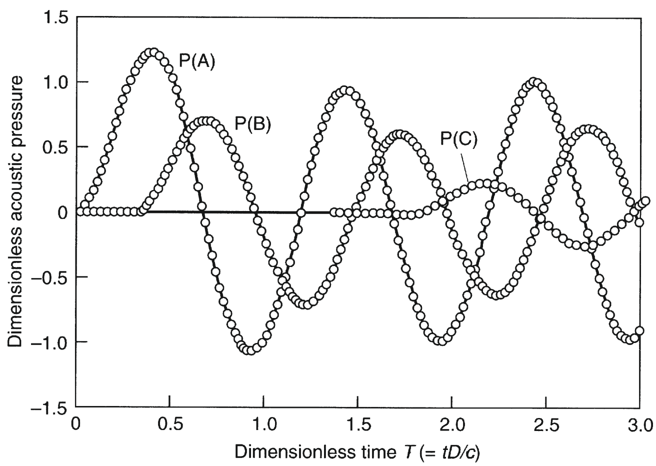


**FIGURE 11.7**

Transient response of a dipole, Astley [66].

More results from the application of infinite elements to transient problems are given by Cipolla and Butler [79], who created a transient version of the Burnett infinite element. There appear to be more difficulties with such elements than with the wave envelope elements, and a consensus that the latter are better for transient problems seems to be emerging. Dampers and boundary integrals can also be used for transient problems. Space is not available to survey these fields, but the reader is directed, again, to Givoli [23] and Geers [24]. One set of interesting results was obtained using transient dampers by Thompson and Pinsky [80].

## 11.12 Linking to exterior solutions (or DtN mapping)

A general methodology for linking finite elements to exterior solutions was proposed by Zienkiewicz et al. [81,82], following various *ad hoc* developments, and this is also discussed in Ref. [12], particularly in Chapter 11. The linking of interior and exterior solutions is also sometimes called *Dirichlet to Neumann* or DtN mapping. Under this title it is discussed by many authors, including Givoli [23]. The exterior solution can take any form, and those chiefly used are (a) exterior series solutions and (b) exterior boundary integrals, although others are possible. The two main innovators in these cases were Berkhoff [10,83], for coupling to boundary integrals, and Chen and Mei [45,46], for coupling to exterior series solutions (although there are earlier papers on the linking of finite elements and exterior solutions). Astley [84] demonstrates for the wave equation that the Chen and Mei methods are effectively the same as what has been more recently termed DtN mapping. Although the methods which have been proposed for linking finite elements to exterior series solutions and boundary integrals are quite different in detail, it is useful to cast them in the same general form. More details of this procedure are given in Ref. [81]. Basically the energy functional given in Eq. (11.13) is again used. If the functions used in the exterior automatically satisfy the wave equation, then the contribution on the boundary reduces to a line integral of the form

$$\Pi = \frac{1}{2}\int_\Gamma \eta \frac{\partial \eta}{\partial n} \mathrm{d}\Gamma \tag{11.33}$$

It can be shown [16,81,82] that if the free parameters in the interior and exterior are **b** and **a**, respectively, the coupled equations can be written as

$$\begin{bmatrix} \mathbf{K} & \bar{\mathbf{K}}^{\mathrm{T}} \\ \bar{\mathbf{K}} & \check{\mathbf{K}} \end{bmatrix} \begin{Bmatrix} \mathbf{a} \\ \mathbf{b} \end{Bmatrix} + \begin{Bmatrix} \mathbf{f} \\ \mathbf{0} \end{Bmatrix} = \begin{Bmatrix} \mathbf{0} \\ \mathbf{0} \end{Bmatrix} \tag{11.34}$$

where

$$\check{K}_{ji} = \tfrac{1}{2}\int_\Gamma [(PN_j)N_i + N_j(PN_i)]\mathrm{d}\Gamma \quad \text{and} \quad \bar{K}_{ji} = \int_\Gamma [(PN_j)(\bar{N}_i)\mathrm{d}\Gamma \tag{11.35}$$

In the above $P$ is an operator giving the normal derivative, i.e., $P \equiv \partial/\partial n$, $\bar{\mathbf{N}}$ is the finite element shape function, $\mathbf{N}$ is the exterior shape function, and $\mathbf{K}$ corresponds to the normal finite element matrix. The approach described above can be used with any suitable form of exterior solution, as we will see. All the nodes on the boundary become coupled.

### 11.12.1 Linking to boundary integrals

Berkhoff [10,83] adopted the simple expedient of identifying the nodal values of velocity potential obtained using the boundary integral, with the finite element nodal values. This leads to a rather clumsy set of equations, part symmetrical, real and banded, and part unsymmetrical, complex and dense. The direct boundary integral method for the Helmholtz equation in the exterior leads to a matrix set of equations

$$\mathbf{A}\tilde{\eta} = \mathbf{B}\frac{\partial \tilde{\eta}}{\partial n} \tag{11.36}$$

(The indirect boundary integral method can also be used.) The values of $\eta$ and $\partial\eta/\partial n$ on the boundary are next expressed in terms of shape functions, so that

$$\eta \approx \hat{\eta} = \mathbf{N}\tilde{\eta} \quad \text{and} \quad \frac{\partial \eta}{\partial n} \approx \frac{\partial \hat{\eta}}{\partial n} = \mathbf{M}\left\{\frac{\partial \tilde{\eta}}{\partial n}\right\} \tag{11.37}$$

$\mathbf{N}$ and $\mathbf{M}$ are equivalent to $\mathbf{N}$ in the previous section. Using this relation, the integral for the outer domain can be written as

$$\Pi = \frac{1}{2}\int_\Gamma \frac{\partial \tilde{\eta}}{\partial n}\mathbf{M}^{\mathrm{T}}\mathbf{N}\tilde{\eta}\,\mathrm{d}\Gamma \tag{11.38}$$

where $\Gamma$ is the boundary between the finite elements and the boundary integrals. The normal derivatives can now be eliminated, using the relation (11.36), and $\eta$ can be identified with the finite element nodal values, $\eta$, to give

$$\Pi = \tfrac{1}{2}\mathbf{b}^{\mathrm{T}}(\mathbf{B}^{-1}\mathbf{A})^{\mathrm{T}}\int_\Gamma \mathbf{M}^{\mathrm{T}}\mathbf{N}\,\mathrm{d}\Gamma\,\mathbf{b} \tag{11.39}$$

Variations of this functional with respect to $\mathbf{b}$ can be set to zero, to give

$$\frac{\partial \Pi}{\partial \mathbf{b}} = \frac{1}{2}\left\{(\mathbf{B}^{-1}\mathbf{A})\int_\Gamma \mathbf{M}^{\mathrm{T}}\mathbf{N}\,\mathrm{d}\Gamma + \left[(\mathbf{B}^{-1}\mathbf{A})\int_\Gamma \mathbf{M}^{\mathrm{T}}\mathbf{N}\,\mathrm{d}\Gamma\right]^{\mathrm{T}}\right\}\mathbf{b} = \check{\mathbf{K}}\mathbf{b} \tag{11.40}$$

where $\check{\mathbf{K}}$ is a "stiffness" matrix for the exterior region. It is symmetric and can be created and assembled like any other element matrix. The integrations involved must be carried out with care, as they involve singularities. Results obtained for the problem of waves refracted by a parabolic shoal are shown in Fig. 5.6 of Ref. [82].

### 11.12.2 Linking to series solutions

Chen and Mei [45,46] took the series solution for waves in the exterior, and worked out explicit expressions for the exterior and coupling matrices, $\bar{\mathbf{K}}$ and $\hat{\mathbf{K}}$, for piecewise linear shape functions, $\bar{\mathbf{N}}$, in the finite elements. The series used in the exterior consists of Hankel and trigonometric functions which automatically satisfy the Helmholtz equation and the radiation condition:

$$\eta = \sum_{j=0}^{m} H_j(kr)(\alpha_j \cos j\theta + \beta_j \sin j\theta) \tag{11.41}$$

The method described above leads to the following matrices:

$$\bar{\mathbf{K}}^{\mathrm{T}} = \frac{-knL_c}{2}\begin{bmatrix} 2H_0' & \cdots & H_n'(\cos n\theta_p + \cos n\theta_1) & H_n'(\sin n\theta_p + \sin n\theta_1) & \cdots \\ 2H_0' & \cdots & H_n'(\cos n\theta_1 + \cos n\theta_2) & H_n'(\sin n\theta_1 + \sin n\theta_2) & \cdots \\ 2H_0' & \cdots & H_n'(\cos n\theta_2 + \cos n\theta_3) & H_n'(\sin n\theta_2 + \sin n\theta_3) & \cdots \\ \vdots & \cdots & \vdots & \vdots & \ddots \\ 2H_0' & \cdots & H_n'(\cos n\theta_{p-1} + \cos n\theta_p) & H_n'(\sin n\theta_{p-1} + \sin n\theta_p) & \cdots \end{bmatrix} \tag{11.42}$$

$$\hat{\mathbf{K}} = \pi rkh\left\{\mathrm{diag}[2H_0H_0' \;\; H_1'H_1 \;\; H_1'H_1 \;\; \cdots \;\; H_s'H_s \;\; H_s'H_s]\right\} \tag{11.43}$$

where $m$ is the number of terms in the Hankel function series, $r$ is the radius of the boundary, $L_c$ is the distance between the equidistant nodes on $\Gamma_C$, $p$ is the number of nodes, and $H_n$ and $H_n'$ are Hankel functions and derivatives evaluated with argument $(kr)$.

Other authors have worked out the explicit forms of the above matrices for linear shape functions, and it is possible to work them out for any type of shape function, using, if necessary, numerical integration. It will be noticed that the matrix $\hat{\mathbf{K}}$ is diagonal. This is because the boundary $\Gamma_B$ is circular and the Hankel functions are orthogonal. If a noncircular domain is used, $\hat{\mathbf{K}}$ will become dense. Chen and Mei [45] applied the method very successfully to a range of problems, most notably that of resonance effects in an artificial offshore harbor, the results for which are shown in Chapter 12, Fig. 12.6 of Ref. [12].

The method was also utilized by Houston [85], who applied it to a number of real problems, including resonance in Long Beach harbor, shown in Fig. 11.8.

## 11.13 Three-dimensional effects in surface waves

As has already been described, when the water is deep in comparison with the wavelength, the shallow-water theory is no longer adequate. For constant or slowly varying depth, Berkhoff's theory is applicable. Also the geometry of the problem may necessitate another approach. The flow in the body of water is completely determined by the conservation of mass, which in the case of incompressible flow reduces to Laplace's equation. The free surface condition is zero pressure. On using Bernoulli's equation and the kinematic condition, the free surface condition can be expressed, in terms of

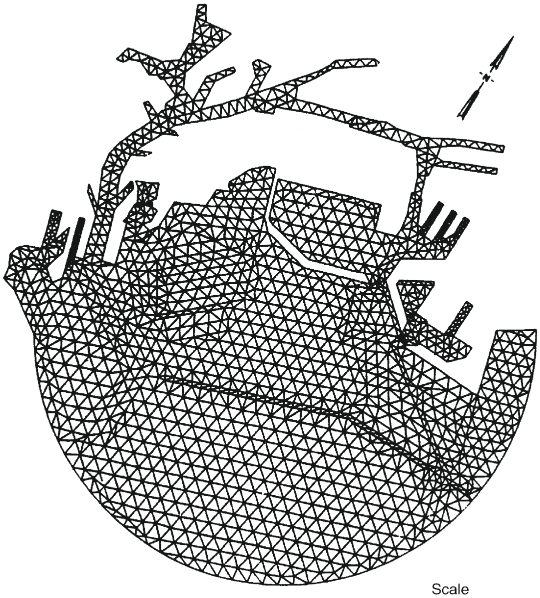


**FIGURE 11.8**

Finite element mesh and wave height magnification for Long Beach Harbor, Houston [85]: (a) finite element grid, grid 3; (b) contours of wave height amplification, grid 3, 232 s wave period.

the velocity potential, $\phi$, as

$$\frac{\partial^2\phi}{\partial t^2} + g\frac{\partial\phi}{\partial t} + 2(\nabla\phi)^{\mathrm{T}}\left[\nabla\left(\frac{\partial\phi}{\partial t}\right)\right] + \tfrac{1}{2}(\nabla\phi)^{\mathrm{T}}\nabla[(\nabla\phi)^{\mathrm{T}}\nabla\phi] = 0 \tag{11.44}$$

where the velocities are $u_i = \partial\phi/\partial x_i$. This condition is applied on the free surface, whose position is unknown *a priori*. If only linear terms are retained, Eq. (11.44) becomes, for transient and periodic problems

$$\frac{\partial^2\phi}{\partial t^2} + g\frac{\partial\phi}{\partial z} = 0 \quad \text{or} \quad \frac{\partial\phi}{\partial z} = \frac{\omega^2}{g}\phi \tag{11.45}$$

which is known as the *Cauchy-Poisson* free surface condition. It was derived in terms of pressure as Eq. (18.13) of Chapter 18 of Ref. [17]. Three-dimensional finite elements can be used to solve such problems. The actual three-dimensional element is very simple, being a potential element of the type described in Chapter 7 of Ref. [17] or Chapter 5 of Ref. [12]. The natural boundary condition is $\partial\phi/\partial n = 0$, where $n$ is the outward normal, so to apply the free surface condition it is only necessary to add

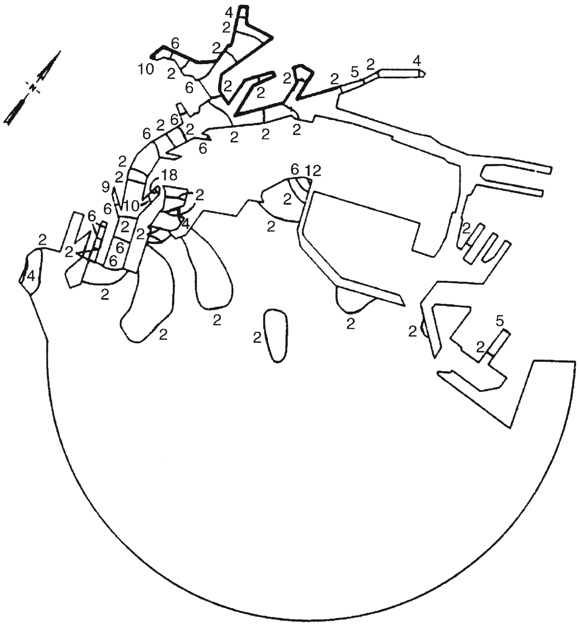

**(b)**

**FIGURE 11.8**

(*Continued*)

a surface integral to generate the $\omega^2/g$ term from the Cauchy-Poisson condition (see Eq. (18.13) of Ref. [17]). Two-dimensional elements in the far field can be linked to three-dimensional elements in the near field around the object of interest. Such models will predict velocity potentials, pressures throughout the fluid, and wave elevations. They can also be used to predict fluid-structure interaction. All the necessary equations are given in Chapter 18 of Ref. [17]. More details of fluid-structure interactions of this type are given by Zienkiewicz and Bettess [86]. Essentially the fluid equations must be solved for incident waves, and for motion of the floating body in each of its degrees of freedom (usually six). The resulting fluid forces, masses, stiffnesses, and damping are used in the equations of motion of the structure to determine its response. Figure 11.9 shows some results obtained by Hara et al. [87] for a floating breakwater. They obtained good agreement between the infinite elements and the methods of Section 11.12.

### 11.13.1 Large-amplitude water waves

There is no complete wave theory which deals with the case when $\eta$ is not small in comparison with the other dimensions of the problem. Various special theories are invoked for different circumstances. We consider two of these, namely, large wave

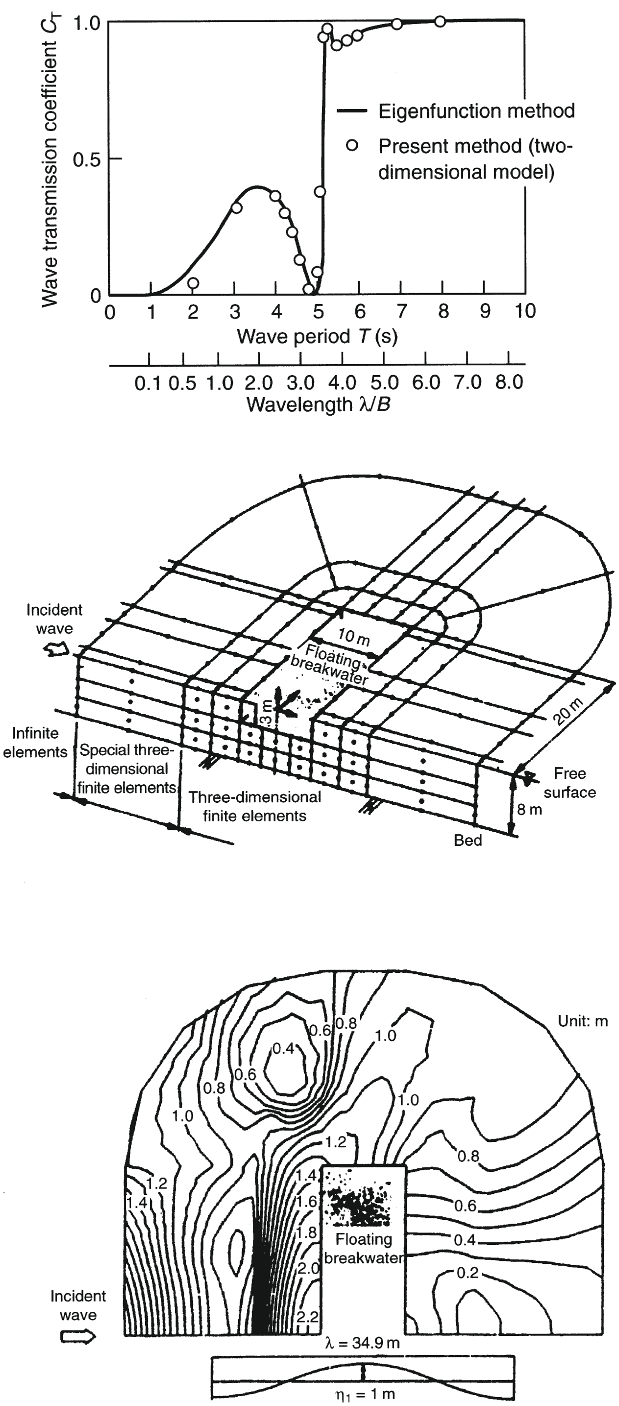


**FIGURE 11.9**

Element mesh, contours of wave elevation, and wave transmission coefficients for floating breakwater, Hara [87].

elevations in shallow water and large wave elevations in intermediate to deep water. We discussed a similar problem in Chapter 10.

### 11.13.2 Cnoidal and solitary waves

The equations modeled in Chapter 10 can deal with large-amplitude waves in shallow water. These are called cnoidal waves when periodic, and solitary waves when the period is infinite. For more details, see Refs. [1–4]. The finite element methodology of Chapter 10 can be used to model the propagation of such waves. It is also possible to reduce the equations of momentum balance and mass conservation to corresponding wave equations in one variable, of which there are several different forms. One famous equation is the Korteweg–de Vries equation, which in physical variables is

$$\frac{\partial \eta}{\partial t} + \sqrt{gH}\left(1 + \frac{3\eta}{2h}\right)\frac{\partial \eta}{\partial x} + \frac{h^2}{6}\sqrt{gH}\frac{\partial^3 \eta}{\partial x^3} = 0 \tag{11.46}$$

This equation has been given a great deal of attention by mathematicians. It can be solved directly using finite element methods, and a general introduction to this field is given by Mitchell and Schoombie [88].

### 11.13.3 Stokes waves

When the water is deep, a different asymptotic expansion can be used in which the velocity potential, $\phi$, and the surface elevation, $\eta$, are expanded in terms of a small parameter, $\varepsilon$, which can be identified with the slope of the water surface. When these expressions are substituted into the free surface condition, and terms with the same order in $\varepsilon$ are collected, a series of free surface conditions is obtained. The equations were solved by Stokes initially, and then by other workers, to very high orders, to give solutions for large-amplitude progressive waves in deep water. There is an extensive literature on these solutions, and they are used in the offshore industry for calculating loads on offshore structures. In recent years, attempts have been made to model the second-order wave diffraction problem, using finite elements, and similar techniques. The first-order diffraction problem is as described in Section 11.8.1. In the second-order problem, the free surface condition now involves the first-order potential.

*First order*

$$\frac{\partial \phi^{(1)}}{\partial z} - \frac{\omega^2}{g}\phi^{(1)} = 0 \tag{11.47}$$

*Second order*

$$\frac{\partial \phi^{(2)}}{\partial z} - \frac{\omega^2}{g}\phi^{(2)} = \alpha_D^{(2)} \tag{11.48}$$

$$\alpha_D^{(2)} = \alpha_{DI}^{(2)} + \alpha_{DD}^{(2)} \quad \text{and} \quad \nu = \frac{\omega^2}{g} \tag{11.49}$$

$$\alpha_{DI}^{(2)} = -\mathrm{i}\frac{\omega}{2g}\phi_D^{(1)}\left(\frac{\partial^2\phi_I^{(1)}}{\partial z^2} - \nu\frac{\partial\phi_I^{(1)}}{\partial z}\right) - \mathrm{i}\frac{\omega}{2g}\phi_I^{(1)}\left(\frac{\partial^2\phi_D^{(1)}}{\partial z^2} - \nu\frac{\partial\phi_D^{(1)}}{\partial z}\right) + \mathrm{i}\frac{2\omega}{g}\nabla\phi_I^{(1)}\nabla\phi_D^{(1)} \tag{11.50}$$

$$\alpha_{DD}^{(2)} = -\mathrm{i}\frac{\omega}{2g}\phi_D^{(1)}\left(\frac{\partial^2\phi_D^{(1)}}{\partial z^2} - \nu\frac{\partial\phi_D^{(1)}}{\partial z}\right) + \mathrm{i}\frac{2\omega}{g}(\nabla\phi_D^{(1)})^2 \tag{11.51}$$

The second-order boundary condition can be thought of as identical to the first-order problem, but with a specified pressure applied over the entire free surface, of value $\alpha$. Now there is no *a priori* reason why such a pressure distribution should give rise to outgoing waves as in the first-order problem, and so the usual radiation condition is not applicable. The conventional procedure is to split the second-order wave into two parts, one the "locked" wave, in phase with the first-order wave, and the other the "free" wave, which is like the first-order wave but at twice the frequency, and with an appropriate wavenumber obtained from the dispersion relation. For further details of the theory, see Clark et al. [89]. Figure 11.10 shows results for the second-order wave elevation around a circular cylinder, obtained by Clark et al. Although not shown, good agreement has been obtained with predictions made by bound-

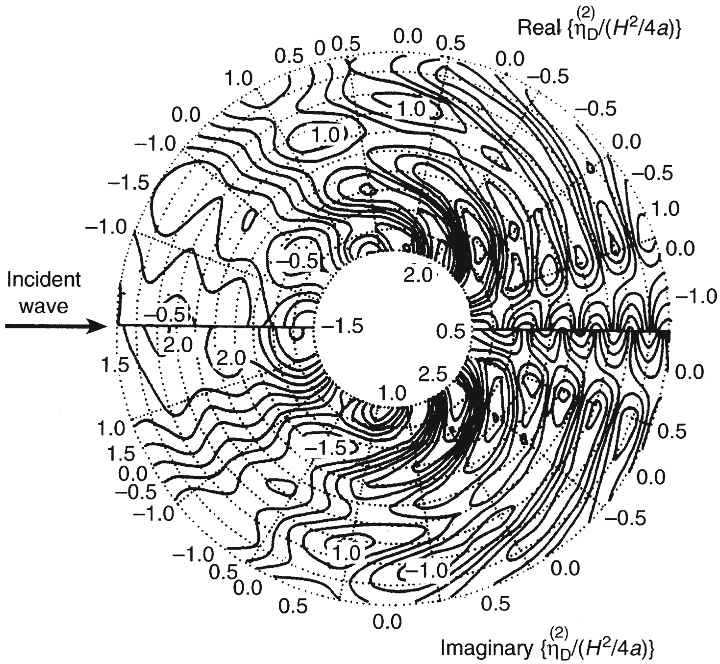


**FIGURE 11.10**
Second-order wave elevations around cylinder—real and imaginary parts, Clark et al. [89].

ary integrals. Preliminary results, for wave forces only, have also been produced by Lau et al. [90]. A much finer finite element mesh is needed to resolve the details of the waves at second order. The second-order wave forces can be very significant for realistic values of the wave parameters (those encountered in the North Sea for example). The first-order problem is solved first and the first-order potential is used to generate the forcing terms in Eqs. (11.50) and (11.51). These values have to be very accurate. In principle the method could be extended to third and higher orders, but in practice the difficulties multiply, and in particular the dispersion relation changes and the waves become unstable [4].

## 11.14 Concluding remarks

For waves which are linear and of medium or large length, compared with the size of the problem, in closed and unbounded domains, finite elements are in a fairly mature state. Improvements in element efficiency, such as spectral methods, which are discussed in Chapter 12, are not so critically important if there are few wavelengths in the problem. Incremental improvements in methods for dealing with the exterior domain continue to be made. As well as higher accuracy from the exterior models, a better mathematical understanding is being obtained. The position is not so well developed in the case of elastic waves, which have not been covered in this chapter, for lack of space. The multiple wave speeds in elasticity make some of the exterior domain methods (discussed in Sections 11.6–11.12) either impossible, or highly complicated in practice. There are some results on error indicators for wave problems, which we could not cover due to lack of space. In general, error indicators do not give such a great payoff as they do in static and potential problems, because usually the waves extend throughout the problem and making the mesh coarse anywhere may have the result of polluting the solution in other regions. See the earlier discussion and that in Chapter 12. Error bounds for the exterior methods are thinner on the ground. Nonlinear waves, such as surface waves of large elevation which have been discussed in Section 11.13, remain a significant challenge. Anyone who has seen a wave break on a shoreline must be aware of how difficult it is to model that process on a computer. But apart from surface waves there are not really that many nonlinear waves of great importance. Effects like shocks arising from bores on water, or shock waves and sonic booms in compressible flow, have been dealt with in other chapters.

## References

[1] H. Lamb, Hydrodynamics, sixth ed., Cambridge University Press, Cambridge, 1932.
[2] G.B. Whitham, Linear and Nonlinear Waves, John Wiley, New York, 1974.
[3] C.C. Mei, The Applied Dynamics of Ocean Surface Waves, Wiley, New York, 1983.

[4] M.J. Lighthill, Waves in Fluids, Cambridge University Press, 1978.
[5] G.M.L. Gladwell, A variational model of damped acousto-structural vibration, J. Sound Vib. 4 (1965) 172–186.
[6] O.C. Zienkiewicz, R.E. Newton, Coupled vibrations of a structure submerged in a compressible fluid, in: Proceedings of the International Symposium on Finite Element Techniques, Stuttgart, 1–15 May 1969, pp. 360–378.
[7] A. Craggs, The transient response of a coupled plate acoustic system using plate and acoustic finite elements, J. Sound Vib. 15 (1971) 509–528.
[8] R.J. Astley, Finite elements in acoustics, in: Proceedings of Inter-noise 98: Sound and Silence: Setting the Balance, Christchurch, New Zealand, vol. 1, 16–18 November 1998, pp. 3–17.
[9] P.M. Morse, H. Feshbach, Methods of Theoretical Physics, McGraw-Hill, New York, 1953.
[10] J.C.W. Berkhoff, Linear wave propagation problems and the finite element method, in: R.H. Gallagher et al. (Eds.), Finite Elements in Fluids, vol. 1, Wiley, Chichester, 1975, pp. 251–280.
[11] O.C. Zienkiewicz, P. Bettess, Infinite elements in the study of fluid structure interaction problems, in: J. Ehlers et al. (Eds.), Proceedings of the Second International Symposium on Computing Methods in Applied Science and Engineering, Versailles, Springer-Verlag, Berlin, 1975 (also published in J. Ehlers et al., Lecture Notes in Physics, vol. 58, Springer-Verlag, Berlin).
[12] O.C. Zienkiewicz, R.L. Taylor, J.Z. Zhu, The Finite Element Method: Its Basis and Fundamentals, seventh ed., Elsevier, Oxford, 2013.
[13] C. Taylor, B.S. Patil, O.C. Zienkiewicz, Harbour oscillation: a numerical treatment for undamped natural modes, Proc. Inst. Civ. Eng. 43 (1969) 141–156.
[14] I. Babuška, F. Ihlenburg, T. Strouboulis, S.K. Gangaraj, A posteriori error estimation for finite element solutions of Helmholtz' equations. Part I: The quality of local indicators and estimators, Int. J. Numer. Methods Eng. 40 (1997) 3443–3462.
[15] I. Babuška, F. Ihlenburg, T. Strouboulis, S.K. Gangaraj, A posteriori error estimation for finite element solutions of Helmholtz' equations. Part II, Int. J. Numer. Methods Eng. 40 (1997) 3883–3900.
[16] O.C. Zienkiewicz, P. Bettess, D.W. Kelly, The finite element method for determining fluid loadings on rigid structures: two- and three-dimensional formulations, in: O.C. Zienkiewicz, R.W. Lewis, K.G. Stagg (Eds.), Numerical Methods in Offshore Engineering, John Wiley, 1978 (Chapter 4).
[17] O.C. Zienkiewicz, R.L. Taylor, J.Z. Zhu, The Finite Element Method: Its Basis and Fundamentals, sixth ed., Elsevier, Oxford, 2005.
[18] A. Bayliss, M. Gunzberger, E. Turkel, Boundary conditions for the numerical solution of elliptic equations in exterior regions, ICASE, Report No. 80–1, 1980.
[19] A. Bayliss, M. Gunzberger, E. Turkel, Boundary conditions for the numerical solution of elliptic equations in exterior regions, SIAM J. Appl. Math. 42 (1982) 430–451.

[20] A. Sommerfeld, Theorie mathematique de la diffraction, Math. Ann. 47 (1896) 317–374.

[21] A. Sommerfeld, Partial Differential Equations in Physics, Academic Press, New York, 1949.

[22] J.A. Bettess, P. Bettess, A new mapped infinite wave element for general wave diffraction problems and its validation on the ellipse diffraction problem, Comput. Methods Appl. Mech. Eng. 164 (1998) 17–48.

[23] D. Givoli, Numerical Methods for Problems in Infinite Domains, Elsevier, Amsterdam, 1992.

[24] T.L. Geers (Ed.), Computational Methods for Unbounded Domains, Kluwer Academic Publishers, Dordrecht, 1998.

[25] F. Ihlenburg, Finite Element Analysis of Acoustic Scattering, Springer, New York, 1998.

[26] K. Bando, P. Bettess, C. Emson, The effectiveness of dampers for the analysis of exterior wave diffraction by cylinders and ellipsoids, Int. J. Numer. Methods Fluids 4 (1984) 599–617.

[27] T.H. Havelock, The pressure of water waves on a fixed obstacle, Proc. Roy. Soc. Lond. A 175 (1950) 409–421.

[28] B. Engquist, A. Majda, Absorbing boundary conditions for the numerical simulation of waves, Math. Comput. 31 (1977) 629–652.

[29] B. Engquist, A. Majda, Radiation boundary conditions for acoustic and elastic wave calculations, Commun. Pure Appl. Math. 32 (1979) 313–357.

[30] R.L. Higdon, Absorbing boundary conditions for difference approximations to the multi-dimensional wave equation, Math. Comput. 47 (176) (1986) 437–459.

[31] R.L. Higdon, Radiation boundary conditions for dispersive waves, SIAM J. Numer. Anal. 31 (1994) 64–100.

[32] T. Hagstrom, T. Warburton, High-order radiation boundary conditions for time–domain electromagnetics using an unstructured discontinuous Galerkin method, in: K. Bathe (Ed.), Computational Fluid and Solid Mechanics, Elsevier, 2003, pp. 1358–1363.

[33] T. Hagstrom, S.I. Hariharan, A formulation of asymptotic and exact boundary conditions using local operators, Appl Numer. Math. 27 (1998) 403.

[34] D. Givoli, High-order nonreflecting boundary conditions without high-order derivatives, J. Comput. Phys. 170 (2001) 849–870.

[35] D. Givoli, B. Neta, High-order non-reflecting boundary scheme for time-dependent waves, J. Comput. Phys. 186 (2003) 24–46.

[36] J. Larsen, H. Dancy, Open boundaries in short wave simulations – a new approach, Coast. Eng. 7 (1983) 285–297.

[37] J.P. Bérenger, A perfectly matched layer for the absorption of electromagnetic waves, J. Comput. Phys. 114 (1994) 185–200.

[38] J.P. Bérenger, Perfectly matched layer for the FDTD solution of wave-structure interaction problems, IEEE Trans. Antenn. Propag. 44 (1996) 110–117.

[39] T.G. Shepherd, K. Semeniuk, J.N. Koshyk, Sponge layer feedbacks in middle-atmosphere models, J. Geophys. Res. 101 (1996) 23447–23464.

[40] S. Abarbanel, D. Gottlieb, J.S. Hesthaven, Well-posed perfectly matched layers for advective acoustics, J. Comput. Phys. 154 (1999) 266–283.

[41] P. Bettess, Infinite Elements, Penshaw Press, Cleadon, U.K., 1992.

[42] R.J. Astley, Infinite elements for wave problems: a review of current formulations and an assessment of accuracy, Int. J. Numer. Methods Eng. 49 (2000) 951–976.

[43] K. Gerdes, Infinite elements for wave problems, J. Comput. Acoust. 8 (2000) 43–62.

[44] P. Bettess, O.C. Zienkiewicz, Diffraction and refraction of surface waves using finite and infinite elements, Int. J. Numer. Methods Eng. 11 (1977) 1271–1290.

[45] H.S. Chen, C.C. Mei, Oscillations and water forces in an offshore harbour, Technical Report 190, Ralph M. Parsons Laboratory for Water Resources and Hydrodynamics, Massachusetts Institute of Technology, Cambridge, MA, 1974.

[46] H.S. Chen, C.C. Mei, Oscillations and wave forces in a man-made harbor in the open sea, in: Proceedings of the 10th Symposium on Naval Hydrodynamics Office of Naval Research, 1974, pp. 573–594.

[47] O.C. Zienkiewicz, C. Emson, P. Bettess, A novel boundary infinite element, Int. J. Numer. Methods Eng. 19 (1983) 393–404.

[48] O.C. Zienkiewicz, P. Bettess, T.C. Chiam, C. Emson, Numerical methods for unbounded field problems and a new infinite element formulation, in: ASME AMD, vol. 46, New York, 1981, pp. 115–148.

[49] P. Bettess, C. Emson, T.C. Chiam, A new mapped infinite element for exterior wave problems, in: P. Bettess, R.W. Lewis, E. Hinton (Eds.), Numerical Methods in Coupled Systems, John Wiley, Chichester, 1984 (Chapter 17).

[50] O.C. Zienkiewicz, K. Bando, P. Bettess, C. Emson, T.C. Chiam, Mapped infinite elements for exterior wave problems, Int. J. Numer. Methods Eng. 21 (1985) 1229–1251.

[51] R.J. Astley, P. Bettess, P.J. Clark, Letter to the editor concerning ref, Int. J. Numer. Methods Eng. 32 (1991) 207–209.

[52] R.J. Astley, G.J. Macaulay, J.P. Coyette, Mapped wave envelope elements for acoustical radiation and scattering, J. Sound Vib. 170 (1994) 97–118.

[53] L. Cremers, K.R. Fyfe, J.P. Coyette, A variable order infinite acoustic wave envelope element, J. Sound Vib. 171 (1994) 483–508.

[54] L. Cremers, K.R. Fyfe, On the use of variable order infinite wave envelope elements for acoustic radiation and scattering, J. Acoust. Soc. Am. 97 (1995) 2028–2040.

[55] D.S. Burnett, A three-dimensional acoustic infinite element based on a prolate spheroidal multipole expansion, J. Acoust. Soc. Am. 95 (1994) 2798–2816.

[56] D.S. Burnett, R.L. Holford, Prolate and oblate spheroidal acoustic infinite elements, Comput. Methods Appl. Mech. Eng. 158 (1998) 117–141.

[57] D.S. Burnett, R.L. Holford, An ellipsoidal acoustic infinite element, Comput. Methods Appl. Mech. Eng. 164 (1998) 49–76.

[58] R.J. Astley, W. Eversman, A note on the utility of a wave envelope approach in finite element duct transmission studies, J. Sound Vib. 76 (1981) 595–601.

[59] R.J. Astley, Wave envelope and infinite elements for acoustical radiation, Int. J. Numer. Methods Fluids 3 (1983) 507–526.

[60] P. Bettess, A simple wave envelope element example, Commun. Appl. Numer. Methods 3 (1987) 77–80.

[61] K. Gerdes, L. Demkowitz, Solution of 3D Laplace and Helmholtz equation in exterior domains of arbitrary shape, using hp-finite-infinite elements, Comput. Methods Appl. Mech. Eng. 137 (1996) 239–273.

[62] L. Demkowitz, K. Gerdes, Convergence of the infinite element methods for the Helmholtz equation in separable domains, Numer. Math. 79 (1998) 11–42.

[63] L. Demkowitz, K. Gerdes, The conjugated versus the unconjugated infinite element method for the Helmholtz equation in exterior domains, Comput. Methods Appl. Mech. Eng. 152 (1998) 125–145.

[64] J.J. Shirron, Solution of Exterior Helmholtz Problems Using Finite and Infinite Elements, Ph.D. Thesis, University of Maryland, 1995.

[65] J.J. Shirron, I. Babuška, A comparison of approximate boundary conditions and infinite element methods for exterior Helmholtz problems, Comput. Methods Appl. Mech. Eng. 164 (1998) 121–139.

[66] R.J. Astley, Mapped spheroidal wave-envelope elements for unbounded wave problems, Int. J. Numer. Methods Eng. 41 (1998) 1235–1254.

[67] R.J. Astley, J.-P. Coyette, Conditioning of infinite element schemes for wave problems, Int. J. Numer. Methods Eng. 17 (2001) 31–41.

[68] D. Dreyer, O. van Estorff, Improved conditioning of infinite elements for exterior acoustics, Int. J. Numer. Methods Eng. 58 (2003) 933–953.

[69] L. Demkowitz, M. Pal, An infinite element for Maxwell's equations, Comput. Methods Appl. Mech. Eng. 164 (1998) 77–94.

[70] I. Harari, P. Barai, P.E. Barbone, Higher-order boundary infinite elements, Comput. Methods Appl. Mech. Eng. 164 (1998) 107–119.

[71] I. Harari, A unified variational approach to domain based computation of exterior problems of time-harmonic acoustics, Appl. Numer. Math. 27 (1998) 417–441.

[72] I. Harari, P. Barai, P.E. Barbone, Numerical and spectral investigations of Trefftz infinite elements, Int. J. Numer. Methods Eng. 46 (1999) 553–577.

[73] I. Harari, P. Barai, P.E. Barbone, M. Slavutin, Three-dimensional infinite elements based on a Trefftz formulation, Comput. Acoust. 9 (2000) 381–394.

[74] R.J. Astley, W. Eversman, Wave envelope elements for acoustical radiation in inhomogeneous media, Comput. Struct. 30 (1988) 951–976.

[75] R.J. Astley, A finite element, wave envelope formulation for acoustical radiation in moving flows, J. Sound Vib. 103 (1985) 471–485.

[76] R.J. Astley, Transient wave envelope elements for wave problems, J. Sound Vib. 192 (1996) 245–261.

[77] R.J. Astley, G.J. Macaulay, J.P. Coyette, L. Cremers, Three dimensional wave-envelope elements of variable order for acoustic radiation and scattering.

Part 1. Formulation in the frequency domain, J. Acoust. Soc. Am. 103 (1998) 49–63.
[78] R.J. Astley, G.J. Macaulay, J.P. Coyette, L. Cremers, Three dimensional wave-envelope elements of variable order for acoustic radiation and scattering. Part 2. Formulation in the time domain, J. Acoust. Soc. Am. 103 (1998) 64–72.
[79] J.L. Cipolla, M.J. Butler, Infinite elements in the time domain using a prolate spheroidal multipole expansion, Int. J. Numer. Methods Eng. 43 (1998) 889–908.
[80] L.L. Thompson, P.M. Pinsky, A space-time finite element method for the exterior structural acoustics problem: time dependent radiation boundary conditions in two space dimensions, Int. J. Numer. Methods Eng. 39 (1996) 1635–1657.
[81] O.C. Zienkiewicz, D.W. Kelly, P. Bettess, The coupling of the finite element method and boundary solution procedures, Int. J. Numer. Methods Eng. 11 (1977) 355–375.
[82] O.C. Zienkiewicz, D.W. Kelly, P. Bettess, Marriage à la mode – the best of both worlds (finite elements and boundary integrals), in: Energy Methods in Finite Element Analysis, Wiley, 1978 (Chapter 5).
[83] J.C.W. Berkhoff, Computation of combined refraction–diffraction, in: Proceedings of the 13th International Conference on Coastal Engineering, Vancouver, 1972, pp. 10–14.
[84] R.J. Astley, Fe mode matching schemes for the exterior Helmholtz problems and their relationship to the FE-DtN approach, Commun. Numer. Methods Eng. 12 (1996) 257–267.
[85] J.R. Houston, Long Beach Harbor: Numerical Analysis of Harbor Oscillations, Vicksburg, MS. Report 1, Misc. Paper h-, US Army Engineering Waterways Experimental Station, 1976.
[86] O.C. Zienkiewicz, P. Bettess, Fluid–structure interaction and wave forces an introduction to numerical treatment, Int. J. Numer. Methods Eng. 13 (1978) 1–16.
[87] H. Hara, K. Kanehiro, H. Ashida, T. Sugawara, T. Yoshimura, Numerical simulation system for wave diffraction and response of offshore structures, Technical Bulletin, TB, October, Mitsui Engineering and Shipbuilding Co., 1983.
[88] A.R. Mitchell, S.W. Schoombie, Finite element studies of solitons, in: P. Bettess, R.W. Lewis, E. Hinton (Eds.), Numerical Methods in Coupled Systems, John Wiley, Chichester, 1984, pp. 465–488 (Chapter 16).
[89] P.J. Clark, P. Bettess, M.J. Downie, G.E. Hearn, Second order wave diffraction and wave forces on offshore structures, using finite elements, Int. J. Numer. Methods Fluids 12 (1991) 343–367.
[90] L. Lau, K.K. Wong, Z. Tam, Nonlinear wave loads on large body by time-space finite element method, in: Proceedings of the International Conference on Computers in Engineering, ASME, New York, 1987, pp. 331–337.